Role of intramolecular dynamics on intermolecular coupling in cyanine dye

T. Virgili,[1,*,†] L. Lüer,[2] G. Cerullo,[2] G. Lanzani,[3] S. Stagira,[2] D. Coles,[4] A. J. H. M. Meijer,[5] and D. G. Lidzey[4,*,‡]
[1]*Istituto di Fotonica e Nanotecnologie–CNR, Piazza L. da Vinci, 32, 20133 Milano, Italy*
[2]*ULTRAS–INFM-CNR, Dipartimento di Fisica, Politecnico di Milano, Piazza Leonardo Da Vinci 32, 20133 Milano, Italy*
[3]*CNST, IIT@POLIMI, Dipartimento di Fisica, Politecnico di Milano, Piazza Leonardo Da Vinci 32, 20133 Milano, Italy*
[4]*Department of Physics and Astronomy, University of Sheffield, Hicks Building, Hounsfield Road, Sheffield S3 7RH, United Kingdom*
[5]*Department of Chemistry, University of Sheffield, Sheffield S3 7HF, United Kingdom*
(Received 6 November 2009; revised manuscript received 23 February 2010; published 15 March 2010)

Using pump-probe spectroscopy with sub-10-fs time resolution, we have studied coherent vibrational dynamics in a cyanine dye, in both monomeric and *J*-aggregate form. We show that coherent excitation of a particular intramolecular vibrational mode can result in a periodic modulation of the intermolecular excitonic coupling within the aggregate. This effect is manifested by a pronounced time-dependent modulation of the electronic transition energy of the aggregate. Such process may have direct importance in a range of electronic processes in supramolecular assemblies.

DOI: 10.1103/PhysRevB.81.125317 PACS number(s): 78.30.Jw, 78.47.jh, 78.47.J−, 78.55.Kz

I. INTRODUCTION

Cooperative electronic phenomena are of significant importance in a variety of different molecular systems. One particularly important example of an electronically coupled molecular excitation can be found in self-assembled *J* aggregates[1,2] in which molecules are arranged in a head-to-tail fashion, resulting in the formation of collective excited states (excitons), having a coherent, delocalized, electronic wave function. *J* aggregates have been extensively studied both experimentally and theoretically as a model system for one-dimensional Frenkel excitons.[3–7] They can also be considered as model systems to explore the chlorophyll aggregates that are central to the process of photosynthesis[8] and as one-dimensional molecular wires.[9] Furthermore, the narrow and redshifted absorption of *J* aggregates has proved to be important for their application in one-dimensional optical microcavities working in the strong coupling regime.[10,11] The relative coupling strength (V) between molecules in a *J* aggregate is an important parameter as it defines the width and energy of the various exciton bands, and will play a part in determining other parameters such as exciton localization and dephasing.[12] While static disorder (inhomogeneous broadening) within an aggregate has a strong influence on its electronic properties, the role of the dynamic properties of the individual molecules within the aggregate is much less clear. Recently the vibronic band structure in the excited state of a jet-cooled dimer[13] has been analyzed using the linear vibronic coupling model[14] confirming the interest in the understanding the role of inter or intramolecular vibrations.

In this paper, we use sub-10-fs pump-probe spectroscopy to study the time-dependent electronic properties of a typical *J*-aggregate-forming dye, both in monomer form and when self-assembled into a *J* aggregate. By comparing the vibrational mode spectra (obtained from the pump-probe measurements) of the aggregated and unaggregated dye, we argue that the strength of intermolecular coupling between molecules in the aggregate can be directly modulated by the coherent excitation of a localized intramolecular vibrational mode associated with the molecules within the aggregate. We believe that this process may also be important in a range of molecular-electronic systems that involve coherent electronic excitations.

II. EXPERIMENTAL METHODS

To study the dynamics of coherent excitations in a *J* aggregate, we have used the cyanine dye 5-chloro-2-[(1E)-2-{[(2Z)-4-chloro-3-(3-sulfonatopropyl)-2,3-dihydro-1,3-benzothiazol-2-ylidene]methyl} prop-1-en-1-yl]3(3sulfonatopropyl)-1,3-benzothiazol-3-IUm (code name NK-2707). This material—whose chemical structure is shown in Fig. 1(a)—was purchased from Hayashibara Ltd. Japan. To prepare an unaggregated monomeric form of NK-2707, the dye was dissolved into a methanol solution (a so-called "good-solvent" for this dye) at a concentration of 0.1 mg/ml. To create *J* aggregates of the NK-2707, it was dissolved at higher concentration (4 mg/ml) into a 5% solution of the biopolymer gelatin dissolved in water. This solution was then spin cast to create a thin film. This rapid increase in dye concentration during this process resulted in the formation of *J*-aggregated molecules of NK-2707 that were suspended in an optically transparent gelatin matrix.

The NK-2707 solutions and thin films were preliminarily characterized using continuous-wave absorption and photoluminescence (PL) spectroscopy. Absorption was measured using a Unicam UV/Vis spectrometer and photoluminescence measured using a charge-coupled device spectrometer following excitation with a GaN laser (409 nm). NK-2707 samples for Raman measurements were prepared by casting a "pure" thin film of the dye (i.e., without the gelatin matrix) onto a glass substrate from a 0.1 mg ml^{-1} methanol solution. Raman spectra were then recorded using a Horiba Jobin Yvon Raman microscope equipped with a 532 nm laser.

Pump-probe measurements were performed using an amplified Ti:sapphire laser producing 500 μJ, 800 nm, 150 fs pulses at 1 kHz. This laser fed a noncollinear optical parametric amplifier (NOPA) pumped by the second harmonic

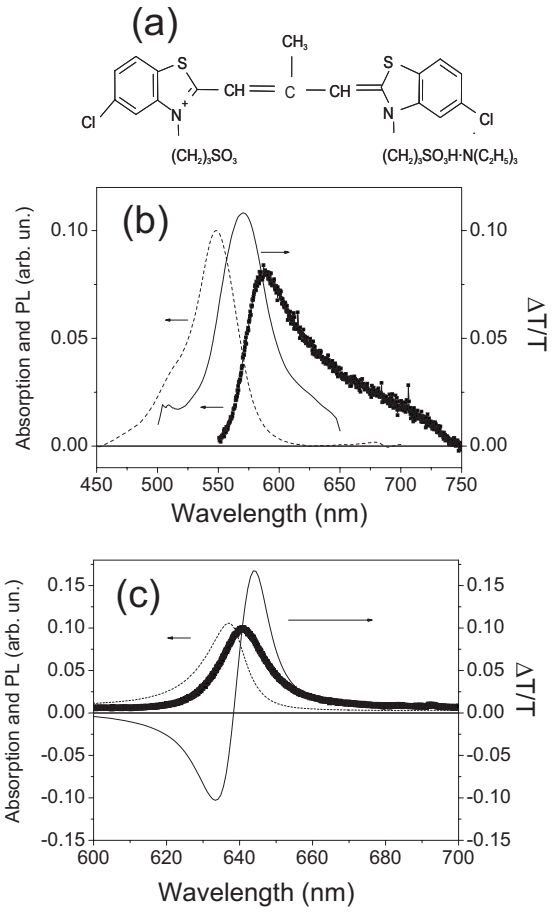

FIG. 1. (a) Chemical structure of cyanine dye NK-2707; (b) ground state absorption (dashed line), photoluminescence (line +symbols), and $\Delta T/T$ spectrum at 100 fs pump-probe delay (solid line) for the NK-2707 monomer in methanol solution; (c) same as (b) for the *J* aggregates.

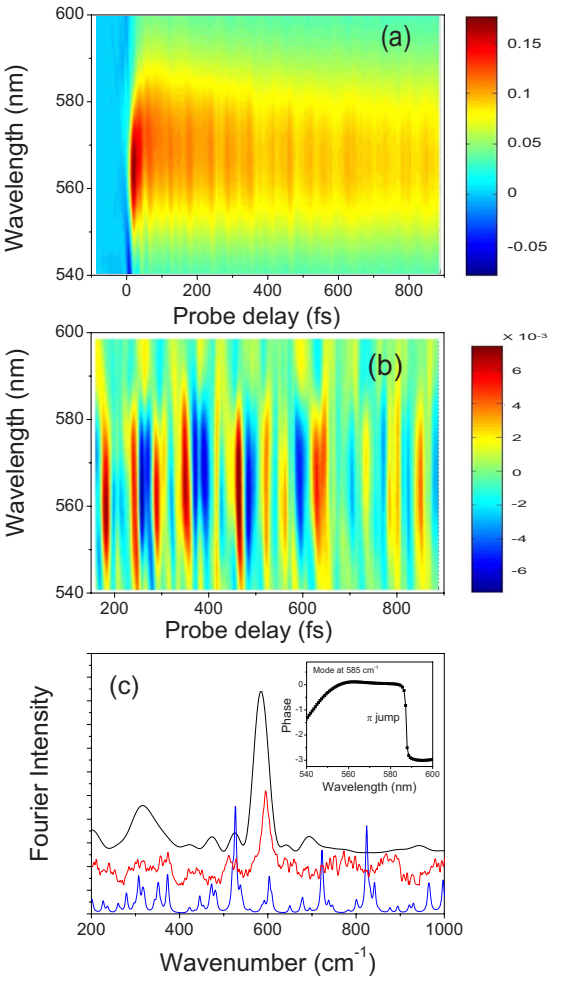

FIG. 2. (Color online) (a) 2D $\Delta T/T(\lambda,\tau)$ map of the dye NK-2707 following excitation by a sub-10-fs pulse; (b) oscillatory component of the signal after subtraction of a slowly varying background; (c) Fourier transform of the $\Delta T/T$ signal recorded at 570 nm (first line from the top, black line), experimental Raman spectrum (second line from the top, red line) and simulated vibrational modes of a NK-2702 monomer (third line from the top, blue line). The inset shows the phase of the mode at 585 cm^{-1} over the spectral range from 540 to 600 nm.

and seeded by a white-light continuum. The NOPA pulses had ultrabroad bandwidth (500–700 nm) and were compressed of sub-10-fs duration by multiple bounces on chirped dielectric mirrors.[15] Measurements were performed in a degenerate pump-probe configuration with parallel polarizations for pump and probe pulses. After transmission through the sample, the probe pulse was then sent to an optical multichannel analyzer capable of single-shot detection at 1 kHz, enabling the acquisition of differential transmission ($\Delta T/T$) spectra, where $\Delta T/T=(T_{off}-T_{on})/T_{off}$, T_{on} and T_{off} being the transmitted probe spectra with and without pump, respectively. Such a technique was used to construct two-dimensional maps $\Delta T/T(\lambda,\tau)$ as a function of both probe wavelength λ and pump-probe delay τ. In all cases, excitation energy densities were lower than 0.1 mJ/cm^2.

The calculation of the NK-2707 Raman modes were performed using the scanning measuring projector version of the Gaussian 03 (Ref. 16) program package with the B3LYP functional method.[17] Calculations were run for the bare anion, its corresponding acid and on the entire ionic complex. For each of these we used various starting geometries.[18]

III. EXPERIMENTAL RESULTS

A. Spectroscopy of the monomer

The stationary absorption and PL spectra of the dye monomer dissolved in a methanol solution are shown in Fig. 1(b) together with the $\Delta T/T$ spectrum recorded at 100 fs probe delay. It can be seen that the dye absorption spectrum consists of a peak at 547 nm and a vibronic shoulder at 508 nm, with the entire spectrum having a linewidth (full width at half maximum) of 40 nm (190 meV). The monomer PL is dominated by an intense peak at 587 nm, with a weakly resolved vibrational replica observed at 690 nm.

Figure 2(a) shows a two-dimensional $\Delta T/T(\lambda,\tau)$ map for the cyanine dye monomer in solution. The $\Delta T/T$ spectrum displays a photoinduced transmission ($\Delta T/T>0$) band that results from the overlap between ground state absorption photobleaching (PB) and stimulated emission (SE) from the

excited state. We find that the $\Delta T/T$ signal undergoes a rapid decay over the first 50 fs (at around 570 nm), consistent with a dynamic shift of 10 nm, followed by a slower decay on the time scale of tens of picoseconds. We believe that the initial redshift is too fast to be attributed to a dynamic Stokes shift resulting from the rearrangement of the solvent around the chromophore,[19] and thus it is likely that it results from a vibrational relaxation to the lowest energetic excited state.[20]We attribute it to vibrational relaxation along another vibrational coordinate which is not directly coupled to the electronic transition. In Fig. 2(a) it is apparent that there is a clear amplitude modulation that is periodic in time superimposed on the slower excited-state dynamics. The oscillatory component of the signal, obtained after subtracting an appropriate decaying background, is shown in Fig. 2(b). Here, the complex pattern observed results from the superposition of several frequencies that correspond to the various vibrational intramolecular modes of the molecule that are coupled to the electronic transition.[21]

In Fig. 2(c), we plot the Fourier transform of the oscillatory component of the signal detected at a probe wavelength of 570 nm (first line from the top, black line). For comparison, we also show the Raman spectrum recorded for a thin film of NK-2707 (second line from the top, red line) and the calculated Raman spectrum of an isolated molecule (third line from the top, blue line). The most intense vibrational mode in the Fourier transform of the pump-probe signal occurs at 585 cm^{-1} (72 meV). This mode is clearly resolved in the Raman spectrum and is reproduced by our calculations and originates from a backbone deformation (see supporting information). In general, there is a reasonable qualitative agreement between the calculated and measured Raman spectra—particularly in the frequency range between 200 to 700 cm^{-1}. It can be seen however that the strong modes predicted at 722 and 827 cm^{-1} are not observed experimentally. As Raman intensities are a third-order property, the predicted intensities of various modes can be very sensitive to the exact details of the model such as basis set size and calculation method. In this particular case however the discrepancy probably results from the treatment of correlation and the problems that density functional theory has with Van der Waals interactions (which are in many cases the major culprits for disparities between theory and experiment). We have measured the phase of the mode at 585 cm^{-1} and find that it evolves smoothly over the whole probe wavelength region, but exhibits an abrupt π jump at a wavelength of 585 nm. Such a π jump identifies the peak of the electronic transition whose energy is modulated by the vibration and is direct evidence for electron-phonon coupling. We note that 585 nm corresponds to the PL emission peak, rather than that of the ground-state absorption. This demonstrates that we are observing an oscillation of the excited-state wave packet around its own equilibrium position. This assignment is consistent with the fact that the mode period ($\approx$57 fs) is much longer than the duration of the pump pulse. Therefore, excitation of ground-state vibrational coherence via the resonant impulsive stimulated Raman scattering mechanism, which requires some motion of the excited-state wave packet during the pump pulse duration, is minimized.

B. Spectroscopy of the *J* aggregate

We now turn our attention to measurements on thin films of *J* aggregates. In Fig. 1(c), we plot the linear absorption and photoluminescence of the *J* aggregate along with a $\Delta T/T$ spectrum (taken at 100 fs probe delay). The linear absorption spectrum peaks at 636 nm (1.95 eV) and has a linewidth of 12 nm (40 meV). Both the narrowing and strong redshift (90 nm or 322 meV) of absorption compared to the unaggregated monomer are well-known characteristics of a *J* aggregated molecular system. The PL spectrum consists of an intense transition at 640 nm (with a linewidth of 40 meV) that is assigned to one-exciton emission. There is no evidence of vibrational structure in both the absorption and emission band of the exciton. This confirms a picture in which the electronic excitation, being delocalized over many molecules, distributes the intramolecular deformation and also suggests a negligible electron-phonon coupling for the intermolecular modes. It can be seen that the $\Delta T/T$ spectrum divides into two distinct regions; from 620 to 640 nm we detect photoinduced absorption (PA) and from 640 to 670 nm we record photoinduced transmission ($\Delta T/T>0$). In our experiments, the pump pulse creates one-exciton states, mostly with quantum number $k=1$, since this transition comprises 81% of the total oscillator strength.[11,22] We thus observe PB of the transition from ground state (g) to the $k=1$ one-exciton state for the duration of the population lifetime of the excitons. In addition to this, SE occurs from the bottom of the one-exciton state to the ground state, and PA occurs from one-exciton to two-exciton states. We note that the apparent shift between the peak of the PB and the linear absorption is due to its overlap with the PA signal.

In Fig. 3(a) we plot the two-dimensional (2D) $\Delta T/T$ map recorded for the *J* aggregate over the wavelength region 620 to 660 nm. The temporal decay of the *J*-aggregate exciton has a fast component with a lifetime of 150 fs and a slower component with a lifetime of around 2 ps, indicating a probable initial bimolecular recombination process due to exciton-exciton annihilation. The oscillatory component of the signal for the *J* aggregate is shown in Fig. 3(b). In contrast to the monomer, it appears more regular indicating the presence of a single dominant oscillatory frequency. This is confirmed by the Fourier transform, displayed in Fig. 3(c), which indicates that a vibrational peak at 320 cm^{-1} dominates the vibrational mode spectrum, with a weaker feature appearing at 260 cm^{-1}. If we compare this spectrum with that of the monomer shown in Fig. 2(c), we see that the peak at 320 cm^{-1} also appears in the monomer spectrum but is relatively weak. The intense mode observed in the monomer at 585 cm^{-1} has apparently weakened considerably in the *J* aggregate. As with the monomer, we also find that the 320 cm^{-1} mode of the *J* aggregate undergoes a π jump, occurring around the point of intersection of the ground-state absorption and PL spectra, which corresponds to the energy of the first excitonic transition, due to the small Stokes shift. Importantly, the appearance of the mode at 320 cm^{-1} in *both* the monomer and the *J* aggregate spectra strongly suggests that it is of intramolecular origin and *does not* correspond to an intermolecular mode (which would anyway be expected to occur at much lower energy).[23] The very strong enhance-

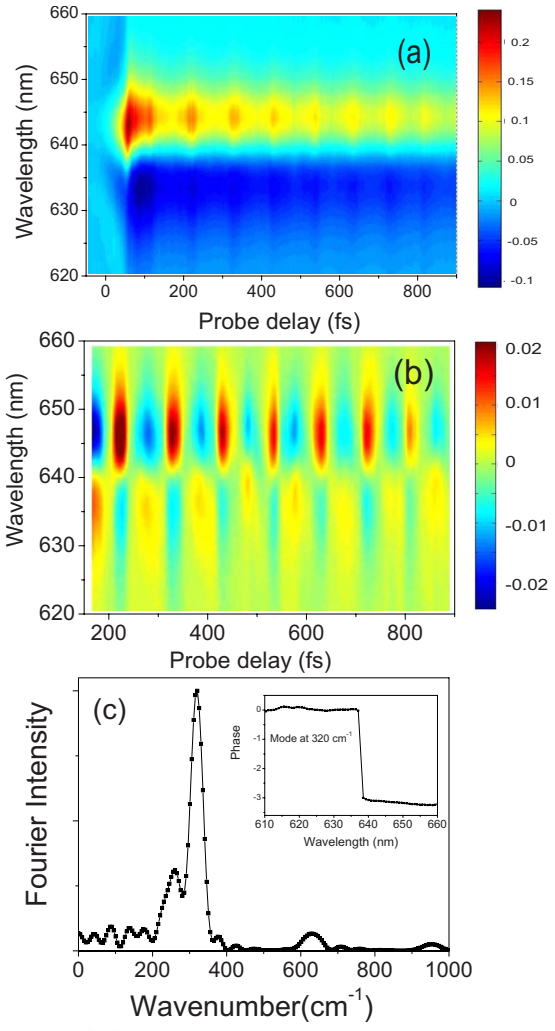

FIG. 3. (Color online) (a) 2D $\Delta T/T(\lambda,\tau)$ map of the dye NK-2707 following excitation by a sub-10-fs pulse; (b) oscillatory component of the signal, after subtraction of a slowly varying background; (c) Fourier transform of the $\Delta T/T$ signal recorded at 570 nm. The inset shows the phase of the mode at 320 cm^{-1} over the spectral range from 610 to 660 nm.

ment of an intramolecular mode in the *J* aggregate thus suggests that we are observing a fundamentally different electron-phonon interaction process than the one occurring in the isolated monomer. Such interpretation is also supported by the appearance in Fig. 3(c) of two minor peaks at the second and third harmonics of the vibrational mode, that are attributed to the nonlinear character of the electron-phonon coupling occurring in the *J* aggregate.

In the following section, we discuss the origin of the apparent enhancement of the dominant vibrational peak and propose a simple model based on a time-dependent modulation of the coupling potential between molecules in the aggregate which is driven by the intramolecular vibrational modes of the cyanine dye molecules. We show that our model is able to qualitatively replicate the experimentally measured pump-probe spectra show in Fig. 3(a).

IV. NUMERICAL MODELING

To understand the very strong apparent enhancement of the vibrational mode at 320 cm^{-1} in the *J* aggregate it is necessary to first determine its molecular origin. To do this, we again use our model of the Raman spectrum of the uncoupled monomer. Our results indicate that there are a number of possible candidate modes around 320 cm^{-1} that can account for the experimentally observed feature. Critically however, the strongest vibrational modes in that region correspond to a backbone wagging/breathing mode that is parallel to and delocalized along the entire molecular backbone (see supplementary information). The resultant motion from this intramolecular mode acts in the same direction as the "end-on-end" electronic-coupling between dipole moments in this class of *J* aggregate. We now make the assumption that this particular intramolecular vibrational mode can produce a time-dependent perturbation of the relative coupling potential between the molecules in the *J*-aggregate lattice [i.e., $V=V(t)$], possibly through a conformational motion that affects their relative intermolecular π overlap. We are confident in the validity of this assumption, as our modeling demonstrates that vibrational coupling to the mode at 320 cm^{-1} results in a cooperative "motion" of the entire molecular backbone and will necessarily result in a time-dependent change in the intermolecular π overlap and thus the coupling constant. It is worth noting that the coupling potential has a nonlinear dependence on the intermolecular distance;[3] as a noticeable consequence, the vibrational modulation of the intermolecular π overlap will result in the appearance of contributions to the electronic response oscillating at the harmonics of the dominant vibrational mode. These harmonics are indeed observed in our measurements and provide the conclusive evidence of the validity of our assumption.

We use the concept of a time-dependent change in the coupling potential to provide a qualitative explanation of the pump-probe spectra shown in Fig. 3(b) as represented schematically in Fig. 4(a). Here, we use the fact that the bleaching of the ground state to the one-exciton band is stationary, representing depletion of ground state population. The energy of the excited-state transitions is time dependent resulting from the modulation of V which we approximate as $V(t)=V_0+\Delta V_1 \sin(\omega_v t)+\Delta V_2 \sin(2\omega_v t)+\Delta V_3 \sin(3\omega_v t)$ where ω_v is the vibrational frequency of the intra-molecular mode and ΔV_1, ΔV_2, and ΔV_3 are the amplitudes of contributions oscillating at the intramolecular frequency and at the first two harmonics. This relation can be interpreted as the series expansion of the coupling potential in terms of the oscillating intermolecular coordinate, arrested to the third power. We consider PB and SE from the $k=1$ one-exciton state to the ground state and PA from the $k=1$ one-exciton state to two-exciton states with quantum numbers (k_1,k_2) (2,1) and (3,2) (note that $k_1 \neq k_2$ as a consequence of the Pauli exclusion principle). The energy Ω of the N states in the one-exciton band can be expressed using

$$\Omega_k = \omega + 2V \cos\left(\frac{\pi k}{N+1}\right). \quad (1)$$

From our best fit, we find that PA mainly occurs to the two lowest two-exciton states optically coupled to the $k=1$ one-

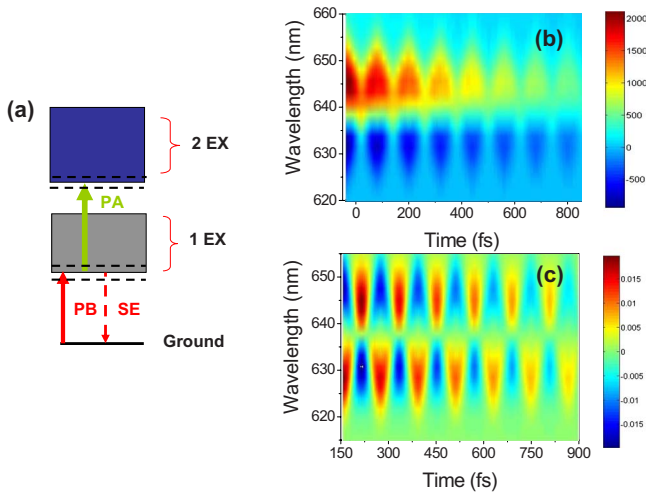

FIG. 4. (Color online) (a) Schematic diagram of the energy levels structure used in our numerical model; (b) simulated 2D $\Delta T/T(\lambda,\tau)$ map of the J aggregate; (c) oscillatory component of the signal in (b).

exciton state. We calculate the energies of these states using $\Omega_{21}=\Omega_2+\Omega_1$ and $\Omega_{32}=\Omega_3+\Omega_2$ [using Eq. (1)], with their dipole moments given by

$$\mu_{gk}=\mu_0\sqrt{\frac{2}{N+1}}\frac{1-(-1)^k}{2}\cot\left[\frac{\pi k}{2(N+1)}\right]. \tag{2}$$

To account for ground state PB, we consider the first three optically allowed transitions from the ground state to one-exciton states with quantum numbers $k=1$, 3, and 5. We also use the fact that the population of each state is proportional to the square of the dipole moment, with the cross section for the transition given by the product of the population and the dipole-moment squared. In each case, we assume the lineshape of the transition to be a Gaussian function $[g(\omega-\Omega)]$ with a linewidth of 150 meV. The contribution to the overall $\Delta T/T$ spectrum of the ground state depletion (which is not affected by coherent vibrational motion) is thus given by

$$\begin{aligned}\mathrm{PB}=&(\mu_{g1})^4 g(\omega-\Omega_{g1})+(\mu_{g1})^2(\mu_{g3})^2 g(\omega-\Omega_{g3})\\&+(\mu_{g1})^2(\mu_{g5})^2 g(\omega-\Omega_{g5}),\end{aligned} \tag{3}$$

where μ_{gk} is the dipole moment of a transition from the ground state (g) to a one-exciton state with quantum number k The other two contributions to the pump-probe spectra are SE and PA, whose time-dependent signals are given by

$$\mathrm{SE}(\omega,t)=(\mu_{g1})^4 g[\omega-\Omega_{g1}(t)] \tag{4}$$

$$\begin{aligned}\mathrm{PA}(\omega,t)=&(\mu_{g1})^2(\mu_{121})^2 g[\omega-\Omega_{121}(t)]\\&+(\mu_{g1})^2(\mu_{132})^2 g[\omega-\Omega_{132}(t)]\end{aligned} \tag{5}$$

in which $\mu_{k_1k_2,k}$ labels the dipole moment of the different transitions, with their energy determined using $\Omega_{121}=\Omega_{21}-\Omega_1$ and $\Omega_{132}=\Omega_{32}-\Omega_1$.

We show our modeled $\Delta T/T$ spectrum in Fig. 4(b). Apart from a slight difference in the shape of the modulation (probably resulting from our approximation of the optical transition as a simple Gaussian function), our model closely replicates the essential features of the experimental pump-probe spectra of the J aggregates shown in Fig. 3(a), validating our approach.

V. DISCUSSION AND CONCLUSIONS

In this work, we have presented an experimental study of the vibrational modes coupled to the electronic transition in a dye both in its monomeric form and as a J aggregate. The results for the monomer in solution are well understood in terms of a traditional picture, in which the pump pulse creates a vibrational wavepacket on the multi-dimensional excited-state potential energy surface. Motion of this wave packet modulates the transient absorption signal (PB and SE) of the probe. For the J aggregate, the situation becomes more complex, since intermolecular couplings become relevant, giving rise to the formation of excitonic bands.

Our combined experimental and modeling studies strongly suggest that intramolecular modes directly modulate the exciton coupling potential in the J aggregate. However, because of the change in the molecular configuration, they cannot strictly be classified as "lattice" (intermolecular) phonons, which would modulate the intermolecular separation. Rather, their effect is to introduce a periodic modulation of the excitonic coupling (V) and thus directly modulate the electronic transition energy. We thus observe an "*electronic*" phenomenon, which is fundamentally different from the "*vibronic*" mechanism characteristic of single molecules, where a vibrational wave packet is created according to the Franck-Condon principle. It is likely that the effects we describe will be found in any molecular system in which direct electromagnetic interactions between coupled chromophores results in the appearance of a modified electronic transition. We believe that a time-dependent modulation of transition energies may have relevance for understanding the microscopic processes at work in a range of molecular-electronic systems and devices, as they are likely to be important in processes that rely on the relative energetic overlap of electronic wave functions. These include both exciton energy-transfer and dissociation via charge transfer. Furthermore, we tentatively suggest that a particular class of intramolecular phonons may modulate the efficiency of charge transport via polaronic or hopping phenomena.

ACKNOWLEDGMENTS

The authors thank D. Polli, G. Gerelli, at the Politecnico di Milano for technical assistance with the pump-probe setup and W. Huang in the Department of Civil and Structural Engineering Sheffield University for the c.w. Raman spectroscopy measurements. Calculation of Raman frequencies were run on the Theoretical Chemistry Group cluster and the central Iceberg cluster at the University of Sheffield.

*Corresponding author.
†tvirgili@polimi.it
‡d.g.lidzey@sheffield.ac.uk

[1] E. E. Jelley, Nature (London) **138**, 1009 (1936).
[2] G. Scheibe, Angew. Chem. **50**, 212 (1937).
[3] *J Aggregates*, edited by T. Kobayashi (World Scientific, Singapore, 1996).
[4] K. Nishimura, E. Tokunaga, and T. Kobayashi, Chem. Phys. Lett. **395**, 114 (2004).
[5] D. J. Heijs, A. G. Dijkstra, and J. Knoester, Chem. Phys. **341**, 230 (2007).
[6] H. Fidder, J. Knoester, and D. A. J. Wiersma, J. Chem. Phys. **95**, 7880 (1991).
[7] H. Fidder and D. A. J. Wiersma, J. Chem. Phys. **98**, 6564 (1993).
[8] W. Kühlbrandt, Nature (London) **374**, 497 (1995).
[9] Z. L. Wang, Adv. Mater. **12**, 1295 (2000).
[10] D. G. Lidzey, T. Virgili, D. D. C. Bradley, M. S. Skolnick, S. Walker, and D. M. Whittaker, Opt. Mater. **12**, 243 (1999).
[11] L. G. Connolly, D. G. Lidzey, R. Butté, A. M. Adawi, D. M. Whittaker, and M. S. Skolnick, Appl. Phys. Lett. **83**, 5377 (2003).
[12] M. Van Burgel, D. A. Wiersma, and K. Duppen, J. Chem. Phys. **102**, 20 (1995).
[13] P. Ottiger, S. Leutwyler, and H. Koppel, J. Chem. Phys. **131**, 204308 (2009).
[14] R. Fulton and M. Gouterman, J. Chem. Phys. **41**, 2280 (1964).
[15] C. Manzoni, D. Polli, and G. Cerullo, Rev. Sci. Instrum. **77**, 023103 (2006).
[16] M. J. Frisch *et al.*, *Gaussian 03, Revision C.02* (Gaussian, Inc., Pittsburgh, PA, 2003).
[17] A. D. Becke, J. Chem. Phys. **98**, 5648 (1993).
[18] See supplementary material at http://link.aps.org/supplemental/10.1103/PhysRevB.81.125317 for more information about the calculation of Raman modes and to see two movies showing the calculated vibrational motion of the molecule undergoing coherent vibrational motion around a frequency of 318 and 609 cm^{-1}.
[19] R. M. Stratt and M. Maroncelli, J. Phys. Chem. **100**, 12981 (1996).
[20] L. Q. Dong, K. Niu, and S. L. Cong, J. Theor. Comput. Chem. **6**, 885 (2007).
[21] G. Lanzani, G. Cerullo, C. Brabec, and N. S. Sariciftci, Phys. Rev. Lett. **90**, 047402 (2003).
[22] J. Knoester and F. C. Spano, in *J Aggregates*, edited by T. Kobayashi (World Scientific Publishing Co. Pte Ltd, Sinapore, 1996).
[23] C. Guo, M. Aydin, H. R. Zhu, and D. L. Akins, J. Phys. Chem. B **106**, 5447 (2002).